Tetrahedron 71 (2015) 3039–3044

Contents lists available at ScienceDirect

Tetrahedron

journal homepage: www.elsevier.com/locate/tet

Binding site of different tannins on a human salivary proline-rich protein evidenced by dissociative photoionization tandem mass spectrometry

Francis Canon [a,b,c,*], Sarah Ployon [a,b,c], Jean-Paul Mazauric [d,e,f], Pascale Sarni-Manchado [d,e,f], Matthieu Réfrégiers [g], Alexandre Giuliani [g,h], Véronique Cheynier [d,e,f]

[a] INRA, UMR1324 Centre des Sciences du Goût et de l'Alimentation, F-21000 Dijon, France
[b] CNRS, UMR6265 Centre des Sciences du Goût et de l'Alimentation, F-21000 Dijon, France
[c] Université de Bourgogne, UMR Centre des Sciences du Goût et de l'Alimentation, F-21000 Dijon, France
[d] INRA, UMR1083 Sciences Pour l'Oenologie, F-34060 Montpellier, France
[e] Montpellier SupAgro, UMR1083 Sciences Pour l'Oenologie, F-34060 Montpellier, France
[f] Université Montpellier I, UMR1083 Sciences Pour l'Oenologie, F-34060 Montpellier, France
[g] Synchrotron SOLEIL, F-91192 Gif Sur Yvette, France
[h] INRA, CEPIA, UAR1008, F-44316 Nantes, France

ARTICLE INFO

Article history:
Received 29 May 2014
Received in revised form 12 October 2014
Accepted 6 November 2014
Available online 13 November 2014

Keywords:
Proline-rich proteins
Tannins
Non-covalent interaction
Binding site
Astringency
Mass spectrometry

ABSTRACT

The sensation of astringency is thought to originate from the interaction occurring between tannins and the salivary proline-rich proteins (PRPs). Astringency perception can be modified by the structure of tannins. Herein, we study the interactions occurring between the human salivary PRP, IB5, and three model tannins with different structure, epigallocatechin gallate and the procyanidin dimers B2 and B2 3′*O*-gallate, using the coupling of mass spectrometry and VUV-synchrotron radiation. The results obtained indicate that the structure of tannins, in particular the degree of polymerization and the galloylation, does not modify the binding site on IB5 involved in the interaction.

1. Introduction

Astringency is a major sensory attribute of wines and especially of red wines,[1] elicited primarily by tannins. It is usually accepted that tannin astringency results from their interaction with salivary proteins and subsequent aggregation and/or precipitation, causing a loss of the lubricating ability of saliva, although it may also involve adsorption of tannins on the oral mucosa.[2–4]

Tannins are ubiquitous in plants and believed to play a role in plant defense against pests and herbivores. Proanthocyanidins, i.e., oligomers and polymers of flavan-3-ols, also called condensed tannins, are the major tannins in foods and beverages, and particularly abundant in grapes and in red wine. They exhibit large structural diversity arising from the presence of several constitutive units and linkage positions, substitution, especially with galloyl groups, and varying degrees of polymerization. These structural features determine tannin properties, including astringency[5,6] and affinity for proteins and peptides that increase with chain length and galloylation[7–10] and are also impacted by tannin conformation.[11]

Among salivary proteins, proline-rich proteins (PRP) are particular prone to interact with tannins.[12] It has been suggested that secretion of PRPs, and especially of basic PRPs, whose only known function is tannin binding, is the first line of defense of herbivores against dietary tannins. Indeed, tannins inhibit digestive enzymes and impede assimilation of dietary proteins and other nutrients. Their binding by PRPs is believed to prevent these processes and could also reduce tannin consumption by triggering astringency. The high affinity of PRPs for tannins is associated to their structural characteristics. PRPs belong to intrinsically disordered proteins, and

* Corresponding author at present address: INRA, UMR CSGA, 17 Rue Sully, F-21065 Dijon Cedex, France. Tel.: +33 3 80 69 35 29; e-mail address: francis.canon@dijon.inra.fr (F. Canon).

http://dx.doi.org/10.1016/j.tet.2014.11.013
0040-4020/

show random coil structure except for small polyproline helix segments. The most accepted model of PRP–tannin interactions describes three different stages as tannin concentration increases: (i) tannins, which are multidentate ligands, bind to several sites on the free protein, (ii) the stoichiometries of the complexes increase and tannins cross-link different protein molecules, (iii) the resulting multimeric aggregates grow until precipitation.

A human salivary PRP, referred to as IB5, and its interactions with tannins have been particularly investigated. Its sequence (Fig. 1A) presents tandem repeats of KPQGPP(P) and eight clusters of 2–5 proline residues. Experiments involving small angle X-ray scattering (SAXS),[13] circular dichroism (CD),[14,15] nuclear magnetic resonance (NMR),[16] and mass spectrometry (MS)[17] have shown that IB5 exhibits a random coil structure and undergoes disorder to order transition upon interaction with epigallocatechin gallate (EgCG), selected as a model tannin ligand.[14,15] Molecular modeling performed on a smaller truncated PRP, $IB9_{37}$, also indicated that structural rearrangement of the peptide occurs during the interaction.[18] Folding of the peptide chain around the tannin, as first proposed by Charlton et al.,[19] may explain the higher tannin affinity of $IB9_{37}$ and IB5 compared to a single proline-rich repeat.

precise binding sites of tannins could not be determined by NMR on full length PRP proteins because of the abundance of proline and repeated sequences. A new method using tandem mass spectrometry coupled to synchrotron radiation as an activation method has recently allowed unambiguous determination of demonstration of binding of the procyanidin dimer B2 3′OG (epicatechin-(4β-8)-epicatechin-3-*O*-gallate, Fig. 1) on the KPQGPPPPPQGG segment of IB5 sequence.[23] In the case of $IB7_{14}$ and $IB9_{37}$, the same three binding sites, corresponding to PP and GG clusters, were involved for all tannin dimers and trimers tested but the binding force was higher for tannins showing extended conformation and longer chain length.[18,11] Once three tannins are linked to the peptide, regardless of its chain length, non-specific cross-linking occurs.[18,11] Similarly, upon, binding with EgCG, the full length protein IB5 forms aggregates with a core structure containing proteins that have bound at least three EgCG molecules and a less dense corona with fewer bound tannins.[21]

Regarding these different observations, it appears important to know if, as for shorter $IB9_{37}$, the same binding site on IB5 is involved in the interaction with tannins having different structures. Therefore, in the present paper, we apply the recent introduced method,

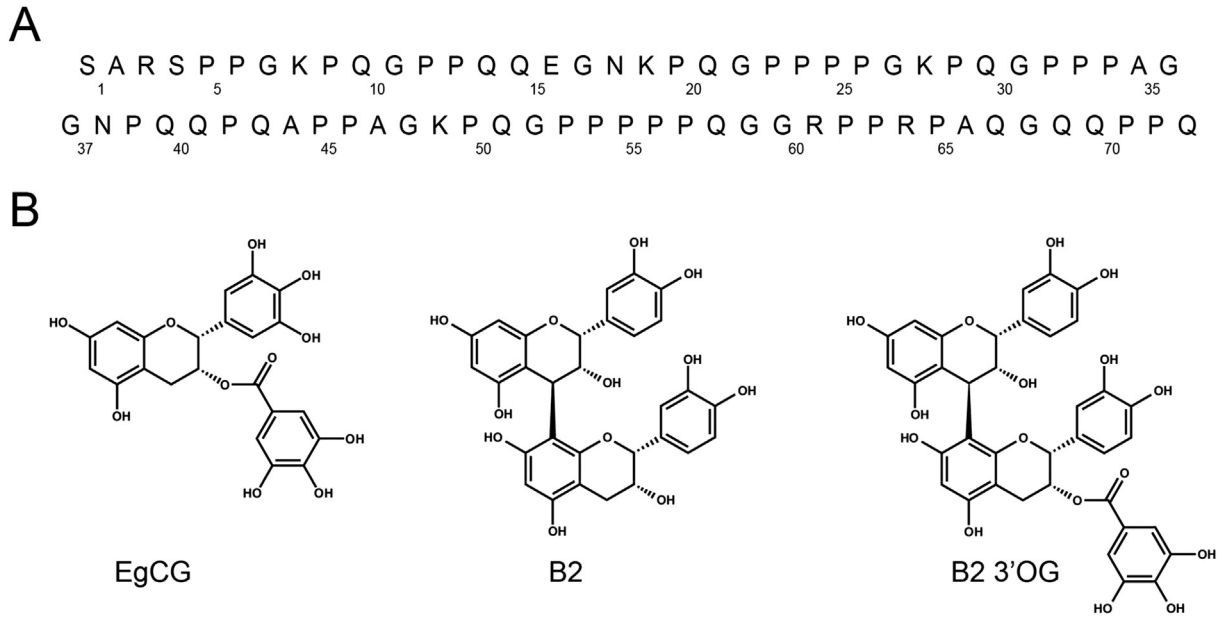

Fig. 1. (A) Sequence of the IB5 human salivary protein. (B) Molecular structure of the epigallocatechin gallate (EgCG), (epicatechin-4β-8)-epicatechin (B2) and epicatechin-(4β-8)-epicatechin-3-*O*-gallate (B2 3′OG).

NMR[20] and a multitechnique approach involving MS and SAXS[21] indicated that at least three EgCG molecules per protein or peptide are required to form PRP–EgCG aggregates. Comparison of different tannins showed that the stability of IB5·tannin complexes increases with the number of hydroxyl groups in the molecule, indicating the involvement of hydrogen bonds.[10] NMR studies performed on two proline-rich peptides ($IB7_{14}$ and $IB9_{37}$) also showed specific hydrophilic interaction at low tannin concentration.[18,11] Mass spectrometry has revealed that IB5·EgCG complexes are present in solution under a distribution of various stoichiometries and fragmentation experiments of complexes with stoichiometries from 1:1 to 1:9 suggested the presence of eight equivalent and independent binding sites on the protein, matching the number of proline clusters.[21] NMR data on complexes of tannins with IB5 or PRP peptides indicated the involvement of Pro and Gly residues in specific non-covalent interactions.[22,18,11,16] However, the coupling MS and vacuum-ultraviolet (VUV) radiation, to localize the binding sites of EgCG and B2 ((epicatechin-4β-8)-epicatechin, Fig. 1B.) on the full PRP, IB5, in 1:1 complexes, and to compare them to that of B2 3′OG.

2. Results and discussion

IB5 is a model of basic salivary PRP, which has been obtained by heterologous expression of the human gene PRB4S in the yeast *Pichia pastoris*.[24] The mass spectrum obtained by electrospraying the protein solution displayed a series of protonated peaks corresponding to four IB5 isoforms with charge states ranging from 5+ to 10+. IB5 isoforms differ from each other by few amino acids at their N-terminal end as previously observed.[23] The sequence of the main isoform is presented in Fig. 1A. Fig. 2A presents a close-up of the mass spectra of IB5 solution and IB5/tannin mixtures for the

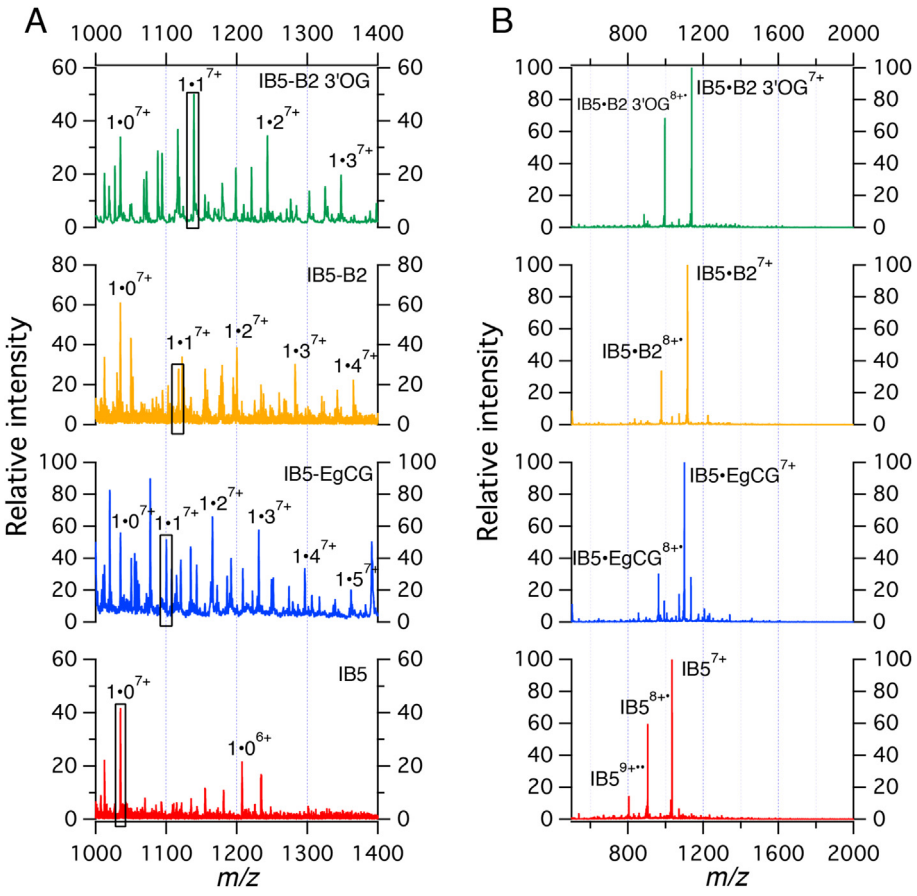

Fig. 2. (A) Electrospray mass spectra of IB5 (bottom line) and IB5/tannins mixtures. Stoichiometries corresponding to the 7+ charge state are labeled. The boxes indicate the stoichiometries selected for subsequent tandem mass spectrometry analysis. (B) DPI tandem mass spectra at 16 eV of the selected precursors.

following tannins: EgCG, B2, B2 3′OG. For each tannin studied here, the corresponding mass spectrum reveals the presence of peaks corresponding to IB5·*n*Tannin complexes with several stoichiometries, as described earlier.[10]

2.1. Mass spectrometry and tandem mass spectrometry analysis of the complexes

In order to localize the binding site of the three tannins on IB5, IB5·1Tannin complexes with the 7+ charge state were selected, and then activated using a 16 eV VUV radiation from a synchrotron radiation beamline. This photon energy has been chosen because of the large sequence coverage and the abundance of fragments it has previously provided on the bare protein.[23] The resulting VUV MS/MS spectra are presented in Fig. 2B. Each spectrum reveals the appearance of the $[M+7H]^{8+\bullet}$ radical cation produced upon the photoionization of the precursor ion. Two regimes of fragmentation have been previously reported using UV and VUV-irradiation.[25] Below the ionization threshold, photon absorption populates electronic excited states, which relax partly through dissociation. This regime, usually referred to as photodissociation, has been shown to lead mainly to the C_α–C bond cleavage. Activation at photon energies above the ionization threshold generates fragments through dissociative photoionization (DPI), with abundant formation of sequence ions of various natures.[26] This regime (DPI) has been shown to provide the highest sequence coverage for IB5 in comparison to the other activation techniques: collision induced dissociation (CID), electron capture dissociation (ECD), and photodissociation (PD).[23]

Comparison of the 16 eV DPI MS/MS spectra of $[IB5{\cdot}1Tannin+7H]^{7+}$ with that of the bare protein ($[IB5+7H]^{7+}$) revealed the presence of peaks shared with the bare proteins (i.e., without retention of the ligand) and of specific peaks that are only present on one spectrum (i.e., that may have retained the ligand). Fig. 3 presents an example of such fragment ions. The x_{48}^{4+} fragment ion of the bare protein is shifted to higher *m*/*z* when associated with the different tannins, as seen in Fig. 3, indicating that the same sequence of the protein is involved for each three tannins.

Analysis of all fragment ions retaining the tannins allows a map of the bound fragments to be established for each $[IB5{\cdot}1Tannin+7H]^{7+}$ precursor ion. The different maps of the fragmentation patterns are presented in Fig. 4 along with that of the bare protein.

For each of the tannins studied here, abundant fragment ions bound with the tannin are revealed upon DPI tandem mass spectrometry. The same experiments performed using ECD has revealed only four fragments retaining B2 3′OG[23] and 0 fragments conserving EgCG (data not shown). We have previously reported that $[IB5{\cdot}B2\ 3'OG+7H]^{7+}$ is more stable than $[IB5{\cdot}EgCG+7H]^{7+}$,[10] which might explain this observation. These observations confirm that DPI is a powerful activation method able to preserve the tannin–protein non-covalent associations. The fragmentation maps obtained for the three tannins show that all fragments from both N- and C-terminal series bearing the tannin ligands contain the QPQAPPAGKPQGPPPPPQGG segment of the sequence.

2.2. Interaction region of the protein with the tannins

This result indicates that this part of the sequence (i.e., QPQAPPAGKPQGPPPPPQGG) is the preferred binding site for EgCG, B2, and B2 3′OG. The sequence identified from the present result

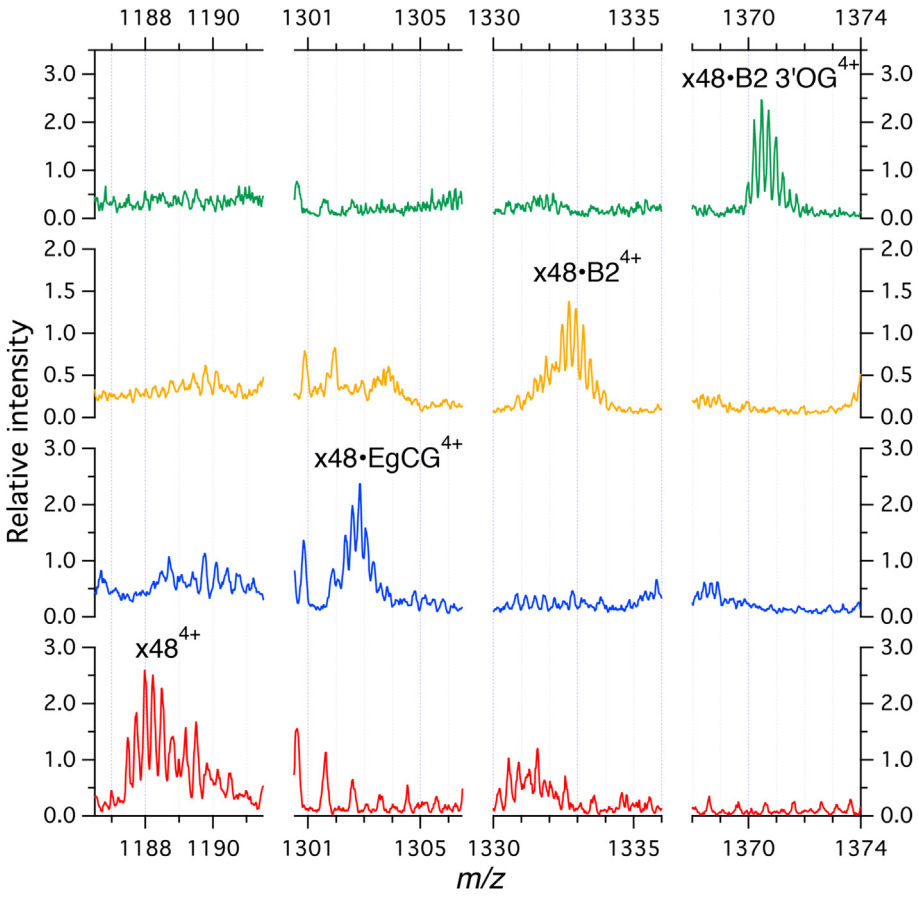

Fig. 3. Close-up of the m/z range corresponding to the x_{48}^{4+} fragment of IB5 (bottom panel) and of the x_{48}^{4+} fragment complexed with EgCG, B2, and B2 3′OG showing the gradual mass shift due to tannin binding on the fragment.

contains the longest cluster of proline, which very likely adopts a PPI or a PPII helix conformation in solution.[27,13,16] Clusters of proline have been previously suggested to be the preferential binding site of tannins on PRPs,[19,16] as this firm segment might provide an initial contact point for the binding.[19,16] Moreover, this segment is surrounded by clusters of glycine and alanine residues, which provide flexible regions allowing establishment of additional hydrogen bonds.[28] The current model of interaction between PRPs and tannins proposes that the clusters of proline are rigid regions, providing initial anchoring points favorable for effective tannin binding. Moreover, the carbonyl function in tertiary amides of proline residues is a more effective hydrogen bond acceptor than that in primary and secondary amides.[29] This firm region are linked by flexible hinges, allowing the reeling of the peptidic chain and the establishment of additional contact points. This model has been proposed to explain that full PRP have higher affinity for tannins as compared to shorter PRP peptides.[18,19] In agreement with this model, ion mobility experiments performed on the IB5·EgCG complexes have shown a transition from an extended conformation to more compact ones upon the binding of tannins,[15] confirming earlier results obtained by NMR and circular dichroism.[16] Molecular modeling calculations have also suggested a notable change in $IB9_{39}$ conformation during its interaction with tannins.[18] Interestingly, this model of interaction seems to be common for IDPs in the binding with their partner.[30] However, the conformational change was not observed with the shorter $IB7_{14}$[27,11] suggesting that it involves folding of the peptide chain around the tannin(s).

Identical sites, involving Pro and Gly residues, have been reported for the binding of three tannins (procyanidin dimers B1 and B3 and trimer C2) on peptides of PRP ($IB9_{37}$ and $IB7_{14}$). The affinity for all tannin molecules increased with the peptide chain length, as observed earlier for IB5[19] while the number of binding sites found for $IB9_{37}$ was slightly lower than for $IB7_{14}$,[18] again suggesting wrapping of the tannin by the PRP chain. The tannin affinity increased with the tannin molecular weight but was also higher for B2 than for the other procyanidin dimers tested, owing to its more extended structure.[18,11] The predominant conformation of B2 3′OG is also more compact than that of B2.[31] Although it does not result in a lower affinity for IB5, as shown by comparing the stability of IB5·tannin complexes,[10] this compact structure, which is able to establish a higher number of hydrogen bonds,[10] probably explains why the binding site of B2 3′OG on the IB5 sequence appears more defined that those of B2 and EgCG.

3. Conclusion

Astringency is an important sensory driver of intrinsic quality of red wines.[1] On one hand, it is known that the structure of tannins, in particular the degree of polymerization and the galloylation, affects astringency.[6] On the other hand, it is generally accepted that salivary PRPs play a role in the astringency sensation due to their ability to interact with tannins. PRP are able to bind several tannins at the same time. Moreover, investigation on interaction between PRP and EgCG have revealed that the proteins, which have bound at least three EgCG molecules connect to each other through EgCG bridges and build PRP·EgCG aggregates.[21] It has been also reported that PRPs undergo a structural rearrangement upon the binding.[15] Herein we investigated the effect of the tannin structure on their binding site onto PRP and we demonstrated that EgCG, B2, and B2 3′OG, which exhibit structural differences, i.e., degree of

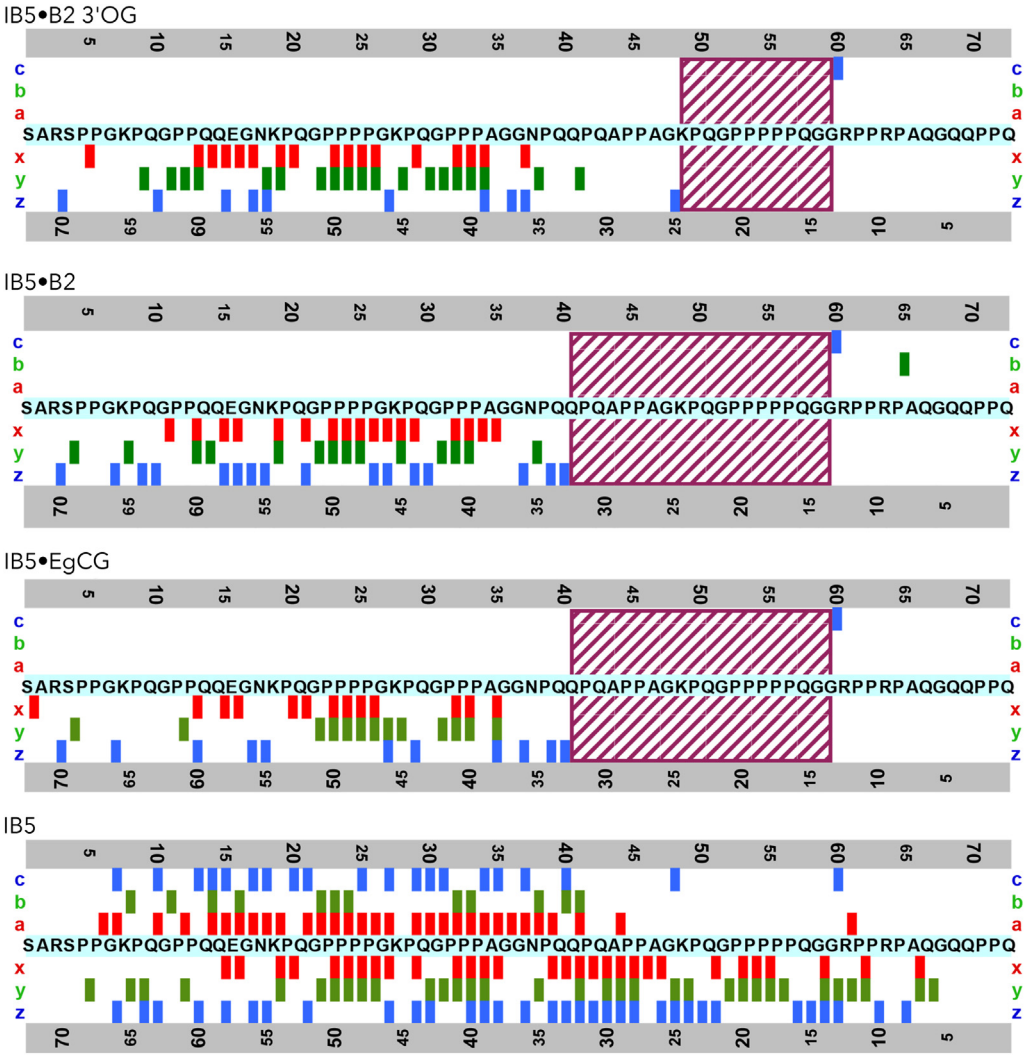

Fig. 4. Fragmentation patterns of IB5 alone and in association with B2 3′OG,[23] B2, and EgCG. The binding sites identified for the tannins on the backbone are indicated by a box.

polymerization and galloylation, bind to the same binding site. This binding site is constituted by a rigid cluster of five proline residues providing an initial contact point, surrounded by flexible hinges allowing structural rearrangements and the establishment of additional hydrogen bonds. Indeed, we previously reported that the structure of tannins modifies the strength of the PRP–tannin interaction as a function of the number of hydroxyl groups of tannins. It is interesting to notice that the structure of tannins affects both the strength of their interactions with PRP and the perception of astringency.[10,6]

4. Experimental section

4.1. Samples

Epigallocatechin gallate (EgCG) has been purchased from Sigma–Aldrich. B2 and B2 3′*O*-gallate were purified as previously described.[32] The human salivary proline-rich protein, IB5, was produced by use of the yeast *P. pastoris* as a host organism and purified as previously described.[13]

Tannin and protein stock solutions were prepared in the following medium: water/ethanol, 88:12 (v/v) acidified at pH 3.3 with acetic acid, mimicking the consumption of red wine.

The stock solutions were diluted to final solutions of 10 μM of IB5 before electrospray analysis. The tannin and protein solutions were mixed at room temperature prior to mass spectrometry analysis to obtain a protein/polyphenol molar ratio of 1:10.

4.2. Mass spectrometry

Mass spectrometry analyses have been performed on linear ion trap fitted with a nanospray ion source (LTQ XL) from Thermo Scientific (San Jose, CA, USA). The mass spectrometer has been coupled to DISCO,[33] a VUV beamline of the SOLEIL synchrotron radiation facility. This coupling is similar to that described previously,[34] with some differences. The APEX branch line was used, with the last stage of the differential pumping system[35] removed. The beamline was set to deliver 16 eV photons with 20 meV energy resolution. An electromechanical shutter was triggered by the activation signal from the mass spectrometer to allow irradiation of the precursor for 2000 ms during the activation stage.

Mass spectra were analyzed using mMass software[36] and Igor Pro (Wavemetrics, Portland, USA).

Acknowledgements

This work was supported by the L' Agence Nationale de la Recherche, France, under the projects ANR-08-BLAN-0065 and ANR-BLAN-0279, and by the Regional Council of Burgundy (FABER AIB 29000622), Européen de Développement Régional (FEDER) (European Union).

References and notes

1. Sáenz-Navajas, M.-P.; Ballester, J.; Pêcher, C.; Peyron, D.; Valentin, D. *Food Res. Int.* **2013**, *54*, 1506–1518.
2. Bajec, M. R.; Pickering, G. J. *Crit. Rev. Food Sci. Nutr.* **2008**, *48*, 858–875.
3. de Freitas, V.; Mateus, N. *Curr. Org. Chem.* **2012**, *16*, 724–746.
4. Gibbins, H. L.; Carpenter, G. H. *J. Texture Stud.* **2013**, *44*, 364–375.
5. Noble, A. C. In *Chemistry of Taste: Mechanisms, Behaviors, and Mimics*; Given, P., Paredes, D., Eds.; American Chemical Society: Washington, DC, 2002; pp 192–201.
6. Vidal, S.; Francis, L.; Guyot, S.; Marnet, N.; Kwiatkowski, M.; Gawel, R.; Cheynier, V.; Waters, E. J. *J. Sci. Food Agric.* **2003**, *83*, 564–573.
7. Sarni-Manchado, P.; Cheynier, V. *J. Mass Spectrom.* **2002**, *37*, 609–616.
8. Poncet-Legrand, C.; Edelmann, A.; Putaux, J.-L.; Cartalade, D.; Sarni-Manchado, P.; Vernhet, A. *Food Hydrocolloids* **2006**, *20*, 687–697.
9. Poncet-Legrand, C.; Gautier, C.; Cheynier, V.; Imberty, A. *J. Agric. Food Chem.* **2007**, *55*, 9235–9240.
10. Canon, F.; Giuliani, A.; Paté, F.; Sarni-Manchado, P. *Anal. Bioanal. Chem.* **2010**, *398*, 815–822.
11. Cala, O.; Pinaud, N.; Simon, C.; Fouquet, E.; Laguerre, M.; Dufourc, E.; Pianet, I. *FASEB J.* **2010**, *24*, 4281–4290.
12. Hagerman, A. E.; Butler, L. G. *J. Biol. Chem.* **1981**, *256*, 4494–4497.
13. Boze, H.; Marlin, T.; Durand, D.; Pérez, J.; Vernhet, A.; Canon, F.; Sarni-Manchado, P.; Cheynier, V.; Cabane, B. *Biophys. J.* **2010**, *99*, 656–665.
14. Pascal, C.; Poncet-Legrand, C.; Imberty, A.; Gautier, C.; Sarni-Manchado, P.; Cheynier, V.; Vernhet, A. *J. Agric. Food Chem.* **2007**, *55*, 4895–4901.
15. Canon, F.; Ballivian, R.; Chirot, F.; Antoine, R.; Sarni-Manchado, P.; Lemoine, J. r. m.; Dugourd, P. *J. Am. Chem. Soc.* **2011**, *133*, 7847–7852.
16. Pascal, C.; Paté, F.; Cheynier, V.; Delsuc, M.-A. *Biopolymers* **2009**, *91*, 745–756.
17. Canon, F.; Paté, F.; Meudec, E.; Marlin, T.; Cheynier, V.; Giuliani, A.; Sarni-Manchado, P. *Anal. Bioanal. Chem.* **2009**, *395*, 2535–2545.
18. Cala, O.; Dufourc, E.; Fouquet, E.; Manigand, C.; Laguerre, M.; Pianet, I. *Langmuir* **2012**, *28*, 17410–17418.
19. Charlton, A. J.; Baxter, N. J.; Lilley, T. H.; Haslam, E.; McDonald, C. J.; Williamson, M. P. *FEBS Lett.* **1996**, *382*, 289–292.
20. Charlton, A. J.; Baxter, N. J.; Lokman Khan, M.; Moir, A. J. G.; Haslam, E.; Davies, A. P.; Williamson, M. P. *J. Agric. Food Chem.* **2002**, *50*, 1593–1601.
21. Canon, F.; Paté, F.; Cheynier, V.; Sarni-Manchado, P.; Giuliani, A.; Pérez, J.; Durand, D.; Li, J.; Cabane, B. *Langmuir* **2013**, *29*, 1926–1937.
22. Baxter, N. J.; Lilley, T. H.; Haslam, E.; Williamson, M. P. *Biochemistry* **1997**, *36*, 5566–5577.
23. Canon, F.; Milosavljević, A. R.; van der Rest, G.; Réfrégiers, M.; Nahon, L.; Sarni-Manchado, P.; Cheynier, V.; Giuliani, A. *Angew. Chem., Int. Ed.* **2013**, *52*, 8377–8381.
24. Pascal, C.; Bigey, F.; Ratomahenina, R.; Boze, H.; Moulin, G.; Sarni-Manchado, P. *Protein Expr. Purif.* **2006**, *47*, 524–532.
25. Bari, S.; Gonzalez-Magana, O.; Reitsma, G.; Werner, J.; Schippers, S.; Hoekstra, R.; Schlatholter, T. *J. Chem. Phys.* **2011**, *134*, 024314–024319.
26. Giuliani, A.; Milosavljevic, A. R.; Canon, F.; Nahon, L. *Mass Spectrom. Rev.* **2014**, *33*, 424–441.
27. Simon, C.; Barathieu, K.; Laguerre, M.; Schmitter, J. M.; Fouquet, E.; Pianet, I.; Dufourc, E. J. *Biochemistry* **2003**, *42*, 10385–10395.
28. Chatterjee, A.; Kumar, A.; Chugh, J.; Srivastava, S.; Bhavesh, N. S.; Hosur, R. V. *J. Chem. Sci.* **2005**, *117*, 3–21.
29. Haslam, E. *J. Nat. Prod.* **1996**, *59*, 205–215.
30. Fuxreiter, M.; Simon, I.; Friedrich, P.; Tompa, P. *J. Mol. Biol.* **2004**, *338*, 1015–1026.
31. Tarascou, I.; Barathieu, K.; Simon, C.; Ducasse, M. A.; Andre, Y.; Fouquet, E.; Dufourc, E. J.; de Freitas, V.; Laguerre, M.; Pianet, I. *Magn. Reson. Chem.* **2006**, *44*, 868–880.
32. Ricardo da Silva, J. M.; Rigaud, J.; Cheynier, V.; Cheminat, A.; Moutounet, M. *Phytochemistry* **1991**, *30*, 1259–1264.
33. Giuliani, A.; Jamme, F.; Rouam, V.; Wien, F.; Giorgetta, J. L.; Lagarde, B.; Chubar, O.; Bac, S.; Yao, I.; Rey, S.; Herbeaux, C.; Marlats, J. L.; Zerbib, D.; Polack, F.; Refregiers, M. *J. Synchrotron Radiat.* **2009**, *16*, 835–841.
34. Milosavljevic, A. R.; Nicolas, C.; Gil, J. F.; Canon, F.; Refregiers, M.; Nahon, L.; Giuliani, A. *J. Synchrotron Radiat.* **2012**, *19*, 174–178.
35. Giuliani, A.; Yao, I.; Lagarde, B.; Rey, S.; Duval, J. P.; Rommeluere, P.; Jamme, F.; Rouam, V.; Wein, F.; De Oliveira, C.; Ros, M.; Lestrade, A.; Desjardins, K.; Giorgetta, J. L.; Laprevote, O.; Herbaux, C.; Refregiers, M. *J. Synchrotron Radiat.* **2011**, *18*, 546–549.
36. Strohalm, M.; Kavan, D.; Novák, P.; Volný, M.; Havlíček, V. *Anal. Chem.* **2010**, *82*, 4648–4651.